Analyst

Combination of the Lateral-Flow Immunoassay with Multicolor Gold Nanorod Etching for the Semi-Quantitative Detection of Digoxin

Journal:	*Analyst*
Manuscript ID	AN-COM-06-2022-001047.R1
Article Type:	Communication
Date Submitted by the Author:	10-Aug-2022
Complete List of Authors:	Bradbury, Daniel; University of California, Los Angeles, Bioengineering Trinh, Jasmine; UCLA, Bioengineering Ryan, Milo; University of California Los Angeles, Bioengineering Chen, Kyle ; University of California, Los Angeles, Bioengineering Battikha, Adel; University of California, Los Angeles, Bioengineering Wu, Benjamin; University of California at Los Angeles, Bioengineering Kamei, Daniel; University of California at Los Angeles, Bioengineering

COMMUNICATION

Combination of the Lateral-Flow Immunoassay with Multicolor Gold Nanorod Etching for the Semi-Quantitative Detection of Digoxin

Received 00th January 20xx,
Accepted 00th January 20xx

DOI: 10.1039/x0xx00000x

Daniel W. Bradbury,[a‡] Jasmine T. Trinh,[a‡] Milo J. Ryan,[a‡] Kyle J. Chen,[a] Adel A. Battikha,[a] Benjamin M. Wu,[a,b] and Daniel T. Kamei [a]*

We are the first to combine the lateral-flow immunoassay (LFA) with gold nanorod (GNR) etching to achieve a multicolor readout where the color produced was correlated with digoxin concentrations in human serum in the relevant range for therapeutic drug monitoring of 0.5-3.0 ng/mL.

1. Introduction

Heart disease, including atrial fibrillation (AF) and heart failure (HF), remains the leading cause of death for adults in the United States. It is expected that the number of individuals with AF in the United States will increase from 5.2 million in 2010 to 12.1 million by the year 2030.[1] Additionally, nearly 6.2 million adults in the United States live with HF and the number of cases is expected to surpass 8 million by the year 2030.[2] Consequently, HF costs the nation an annual $30.7 billion in healthcare services, medications, and missed days of work.[3] Furthermore, cardiovascular disease disproportionately affects underrepresented populations, which are often in areas with reduced healthcare access.[4]

One drug that is used in the treatment of HF and AF is the cardiac glycoside digoxin. Despite being the oldest and one of the most well-known drugs for the treatment of HF and AF, digoxin remains one of the most challenging cardiovascular therapies to administer properly. This is due to its narrow therapeutic window and the small difference between its therapeutic and toxic doses.[5] To address this issue, therapeutic drug monitoring is often employed to measure the blood plasma concentration of the drug and ensure that the trough level is within the therapeutic range of 1-2 ng/mL as opposed to the toxic concentration (>2.8 ng/mL).[6] If the measured concentration of digoxin in the blood is not within the desired range, the patient's next dose can be adjusted, thus providing a method of individualizing treatment. Typically, highly quantitative techniques, such as the enzyme-linked immunosorbent assay (ELISA), high performance liquid chromatography, or automated immunoassay systems, are utilized for monitoring cardiac drugs.[7–9] Despite their success in large hospital settings, these tests are not feasible for use in small mobile clinics residing in medically underserved communities due to the requirement of highly expensive equipment, trained laboratory personnel, and a long time-to-result, especially if the sample has to be sent away to an offsite laboratory.[10]

One effort to make the ELISA more suitable for use in resource-limited settings was the development of the plasmonic enzyme-linked immunosorbent assay (pELISA).[11,12] In the pELISA, traditional chromogenic substrates are replaced with plasmonic nanoparticles. One mechanism involves coupling analyte capture with a reaction that controls the anisotropic etching of gold nanorods (GNRs).[13,14] Different concentrations of the target analyte result in GNRs of different aspect ratios and thus different colored suspensions. This produces a multicolor readout with a full spectrum of colors. Compared to the traditional ELISA, which generates a change in color intensity and thus requires expensive plate readers to interpret results, the pELISA generates a change in color hue. The results are easily interpreted with the naked eye by comparing the color development with a provided reference card (similar to litmus pH test strips). While effective at introducing a semi-quantitative naked-eye readout to the ELISA, the pELISA still has a long time-to-result and requires trained personnel to perform many binding and washing steps, making it unsuitable for use at the point of care (POC). Therefore, there is still a need for a POC device that can perform quantitative therapeutic drug monitoring in underserved communities.

A POC device should be small and lightweight, require minimal power, training, and equipment, and also be low in

[a] *Department of Bioengineering, University of California, Los Angeles, CA 90095 USA*
Email: kamei@seas.ucla.edu
[b] *Division of Advanced Prosthodontics & Weintraub Center for Reconstructive Biotechnology, School of Dentistry, University of California, Los Angeles, CA 90095 USA*
‡ Daniel W. Bradbury, Jasmine T. Trinh, and Milo J. Ryan contributed equally.
Electronic Supplementary Information (ESI) available: See DOI: 10.1039/x0xx00000x

cost. One device that satisfies these criteria is the lateral-flow immunoassay (LFA), a paper-based device that transports a sample via capillary action and uses colorimetric indicators conjugated with antibodies to visually detect the presence or absence of a target analyte. The most recognizable versions of the LFA are the over-the-counter pregnancy test and the COVID-19 rapid antigen tests which have achieved widespread success in today's market due to their ease of use and accurate, rapid results. Despite its success, the LFA still suffers from a few disadvantages which limit its ability to completely replace laboratory-based assays.[15] One disadvantage is that the conventional LFA only provides the user with a qualitative "yes" or "no" binary readout. For this reason, the traditional LFA is not appropriate in situations where a quantitative answer is required, such as therapeutic drug monitoring. Various approaches have been developed to introduce a more quantitative readout to the LFA, such as the barcode-style LFA[16–18] and electronic readers.[19–21] Although these approaches have been useful, the barcode-style LFA has a relatively poor quantitative resolution, while the requirement of electronic readers can increase the cost and complexity of an assay. Thus, there is still a need for inexpensive, easy-to-use, rapid assays that allow for naked-eye quantification of biomarkers at the POC.

In this work, we developed a technology that combines the LFA with the multicolor signal generation capabilities of the pELISA to improve the naked-eye semi-quantitative capabilities of the LFA. In contrast to other approaches that use different colored probes for multiplex detection,[22–24] our approach uses a single color-changing probe to measure concentrations of a single target analyte. Digoxin capture and binding occur on our modified LFA test strip which utilizes platinum nanozyme probes with catalase-like activity. These nanozymes are conjugated to anti-digoxigenin, which is specific to both digoxin and digoxigenin, as digoxigenin is a hapten that shares the same structure as the steroid fraction of digoxin. This test strip is combined with a reaction that controls the oxidative, anisotropic etching of GNRs to produce a wide range of visible colors dependent on the initial digoxin concentration in the sample. Thus, rather than generating changes in color intensity, as conventional LFAs do, our technology generates changes in color hue that are more easily detectable by the naked eye. We demonstrated the potential of this technology to be used for the naked-eye semi-quantification of digoxin in human serum samples within the relevant concentration range for therapeutic drug monitoring of 0.5-3.0 ng/mL. To our knowledge, this is the first reported combination of the LFA with GNR etching, as well as the first multicolor LFA readout where the color hue produced is dependent on the concentration of the antigen analyte.

2. Materials and Methods

2.1 Synthesis of gold nanorods (GNRs)

All reagents and materials were purchased from Sigma-Aldrich (St. Louis, MO) unless otherwise noted. GNRs were synthesized in-house using a modified version of the seeded growth method reported by Ye *et al*.[25] This method requires the preparation of both gold nanoparticle seeds and a growth solution. To make the seed suspension, 5 mL of 0.2 M cetyltrimethylammonium bromide (CTAB) was first prepared by stirring and heating on a hot plate until the CTAB fully dissolved, followed by cooling to 30 °C. Next, under continuous, vigorous stirring at 30 °C, 2.5 mL of filtered ultrapure water (VWR, Radnor, PA) and 2.5 mL of 1 mM $HAuCl_4$ were added into the CTAB solution. This was followed by the addition of 1 mL of freshly prepared 6 mM sodium borohydride. The solution was stirred for 2 min, during which the color changed from yellow to brown, indicating the formation of small gold nanoparticle seeds of approximately 3-4 nm. The seed suspension was left to age for 30 min.

The growth solution was prepared by mixing 180 mg of CTAB and 22 mg of 5-bromosalicylic acid (Tokyo Chemistry Industry America, Portland, OR) in 5 mL of filtered ultrapure water which was heated and stirred until fully dissolved. This solution was cooled to 30 °C, after which 240 µL of 4 mM silver nitrate was added to the growth solution, quickly mixed, and then left undisturbed for 15 min at 30 °C. Next, 5 mL of 1 mM $HAuCl_4$ was added and the solution was stirred with a magnetic stir bar at 800 RPM for 15 min. 40 µL of 64 mM L-ascorbic acid was then vigorously stirred into the solution for 30 s until it became colorless, indicating the reduction of Au(III) to Au(I).

Finally, 4 µL of the aged gold seed suspension was added and stirred for another 30 s. The final suspension was then left to sit undisturbed for at least 12 h, after which the suspension was divided into 2 mL aliquots and centrifuged for 15 min at 8600 RCF and 30 °C. The supernatant was then discarded and each pellet of GNRs was resuspended in 2 mL of filtered ultrapure water. This centrifugation was repeated, and after discarding the supernatant, the final pellets were combined and resuspended to a total volume of 333 µL in filtered ultrapure water for 30-fold concentration.

2.2 Demonstration of GNR etching for multicolor signal generation

The GNR etching precursor suspension for one reaction was made by mixing 8.25 µL of a solution containing 0.1 M CTAB and 0.1 M Tween 20 with 6.75 µL of synthesized GNRs, 22.5 µL of 1.4 M NaBr in 0.2 M citrate buffer (pH 4), and 7.5 µL of 100 µM horseradish peroxidase (HRP) in 0.1 M phosphate buffer (pH 6) in a well of a 96-well plate. To perform the etching reaction, 40 µL of varying concentrations of hydrogen peroxide (H_2O_2) in 3 mM NaOH were mixed into each well containing the GNR etching precursor suspension. After 10 min, photographs were taken with a Nikon D3400 DSLR camera (Nikon, Tokyo, Japan) in a controlled lighting environment and the UV-Vis spectra were observed using a Synergy H1 Hybrid Multi-Mode reader (BioTek, Winooski, VT).

2.3 Synthesis of porous platinum-shell gold-core nanozymes (PtNs)

PtNs were synthesized using a protocol modified from Loynachan *et al*.[26] In a 20 mL scintillation vial, 200 µL of a 20% w/w 10 kDa polyvinylpyrrolidone (PVP) solution was mixed with

10 mL of 0.35 mM 20 nm gold nanoparticles (GNs) (nanoComposix, San Diego, CA) and allowed to incubate for 5 min at room temperature (22°C). 200 µL of a 100 mM chloroplatinic acid solution and 400 µL of a 100 mg/mL L-ascorbic acid solution were then added simultaneously and immediately mixed. The suspension was then allowed to react in a 65 °C oil bath under magnetic stirring at 1200 RPM for 1 h. During this reaction, the platinum ions would be reduced by the L-ascorbic acid and deposit onto the surface of the GNs resulting in the formation of a thick, porous platinum shell. The resulting suspension was cooled in a 25 °C water bath for 1 h. To purify the particles from excess reagents, the suspension was split into 1 mL aliquots. Each aliquot was centrifuged twice at 8600 RCF for 12 min at 4 °C. The supernatant was removed, and the pellets were resuspended in 1 mL of filtered ultrapure water in between the centrifugation cycles. The supernatant from the original aliquot was recovered after both centrifugation cycles and centrifuged separately at the same settings to capture any remaining particles in the supernatant. After the original aliquot and the recovered supernatants were each centrifuged twice, the pellets were combined and resuspended in 500 µL of filtered ultrapure water, effectively doubling the concentration of PtNs relative to the unpurified PtN batch.

2.4 Preparation of anti-digoxigenin antibody-decorated porous platinum-shell gold-core nanozyme probes (anti-digoxigenin PtNPs)

To create anti-digoxigenin PtNPs, 41.5 µL of purified PtNs was first diluted in 458.5 µL of filtered ultrapure water. Next, 2 µL of a 0.1 M sodium borate (pH 9) solution was added to adjust the PtN suspension pH to 7. Subsequently, 0.5 µg of anti-digoxigenin polyclonal antibody was added, and the mixture was allowed to react for 30 min at room temperature (22 °C) to allow the antibodies to adsorb and conjugate onto the surface of the PtNs through a combination of electrostatic interactions, hydrophobic interactions, and dative bonds. This was followed by the addition of 50 µL of a 10% w/v bovine serum albumin (BSA) solution in filtered ultrapure water in order to passivate the surface of the PtNs. After reacting for 10 min, the suspension was purified of free antibodies using three centrifugation cycles at 8600 RCF and 4°C for 6 min each. The pellets resulting from the first two cycles were resuspended in 200 µL of 1% w/v BSA in filtered ultrapure water while the pellet from the final centrifugation cycle was resuspended to a total volume of 25 µL in a 0.06 M sodium borate (pH 9) solution.

2.5 Preparation of BSA-biotin-decorated gold nanoprobes (GNPs)

To create the BSA-biotin-decorated GNPs that bind to the control line, 2 µL of a 0.1 M sodium borate (pH 9) solution was first added to 500 µL of 40 nm GNs (nanoComposix, San Diego, CA) to achieve a pH of 7. Next, 8 µg of BSA-biotin (Thermo Scientific, Waltham, MA) was added to the suspension and incubated for 30 min at room temperature (22°C). Afterward, 50 µL of a 10% w/v BSA solution in filtered ultrapure water was added to the suspension and incubated for an additional 10 min. Free antibodies were then removed from the suspension using three centrifugation cycles at 8600 RCF and 4°C for 6 min each. The pellets resulting from the first two cycles were resuspended in 200 µL of 1% w/v BSA in filtered ultrapure water. The pellet from the final centrifugation cycle was resuspended to a total volume of 50 µL in a 0.07 M sodium borate (pH 9) solution.

2.6 Preparation of test strip for detection of digoxin

Proteins were printed and immobilized on the Unisart CN95 nitrocellulose membrane (Sartorius, Göttingen, Germany) using an Automated Lateral Flow Reagent Dispenser (Claremont BioSolutions LLC, Upland, CA) with the voltage setting at 4.5 V and a Fusion 200 syringe pump (Chemyx Inc, Stafford, TX) with a flow rate of 250 µL/min. The test line was formed by printing a solution of 0.5 mg/mL digoxin-BSA (Fitzgerald Industries International, Acton, MA) in 25% w/v sucrose at two locations that were 1 mm apart with two print cycles each, such that the solution printed merged into one thick test line. The control line was formed by printing a solution of 1 mg/mL polystreptavidin (Biotez, Berlin, Germany) in 25% w/v sucrose with two print cycles. The printed membrane was left in a vacuum-sealed desiccation chamber for 48 h.

To assemble the test strip, the nitrocellulose membrane was first adhered to an adhesive backing and cut into 5 mm wide strips. A 5 mm × 19 mm Standard 17 fiberglass paper (Cytiva, Marlborough, MA) sample pad was placed on the adhesive upstream of the test line and overlapped the nitrocellulose membrane by 2 mm. A 5 mm × 22 mm CF6 (Cytiva, Marlborough, MA) absorbent pad was placed on the adhesive backing downstream of the control line and overlapped the nitrocellulose membrane by 2 mm.

2.7 Semi-quantitative detection of digoxin using the LFA with a multicolor readout

A 60 µL sample containing digoxin spiked into pooled human serum (Innovative Research Inc, Novi, MI) was mixed with 3 µL of anti-digoxigenin PtNPs, 4 µL of BSA-biotin-decorated GNPs, 5 µL of running buffer (4% w/v 10 kDa PVP, 0.4% w/v BSA, 0.4% w/v casein, and 0.4% w/v Tween 20 in 100 mM potassium phosphate buffer, pH 7.2), and 28 µL of Milli-Q water and placed in a 2 mL microcentrifuge tube. The sample pad of the LFA was then dipped into the 2 mL tube. After 7.5 min, an additional 50 µL of chase buffer (0.5% w/v 10 kDa PVP, 0.05% w/v BSA, 0.05% w/v casein, and 0.05% w/v Tween 20 in 12.5 mM potassium phosphate buffer, pH 7.2) was added to the same tube. The LFA was then run for an additional 5 min before photos were taken using a Nikon D3400 digital camera in a controlled lighting environment. Following this antigen capture and detection step, a 5 mm x 5 mm portion of the test strip containing the test line was cut out and taped onto a 3D printed tab. The tab was then placed into a 3D printed holder above a 96-well plate (**Figure S1** in Supplementary Information). This holder positioned the tab in the center of the well with the test line region submerged in the H_2O_2 incubation solution (100 µL of 8 mM H_2O_2 in 3 mM NaOH) within the well. The 96-well plate with the tab was placed on a microplate shaker at 600 RPM for 25

min. 40 µL of the H_2O_2 incubation solution was then transferred into a separate 96-well plate containing the GNR etching precursor solution discussed previously in Section 2.2. After reacting for 10 min, photographs were taken with a Nikon D3400 DSLR digital camera in a controlled lighting environment and the UV-Vis spectra were measured using a Synergy H1 Hybrid Multi-mode reader.

3. Results and Discussion

3.1 Mechanism of the proposed LFA with a semi-quantitative, multicolor readout

In this work, we propose that the LFA could be combined with platinum-shelled nanozymes possessing catalase-like activity and the anisotropic etching of GNRs to produce a multicolor readout that is dependent on the concentration of the target analyte, digoxin, in a human serum sample. This would allow for naked-eye biomarker semi-quantification without the need for electronic readers or complex and expensive laboratory equipment. The general assay procedure and mechanism are detailed in **Figure 1**. The serum sample is first mixed with the anti-digoxigenin PtNPs. The anti-digoxigenin antibodies conjugated onto the surface of the nanozymes are specific to both digoxin and digoxigenin, which is the steroid fraction of digoxin. Therefore, the anti-digoxigenin PtNPs capture any digoxin in the serum sample. Increasing concentrations of digoxin in the serum result in increased capture and thus greater saturation of the antibodies on the nanozyme surface.

After the sample is applied to the LFA test strip, it flows from the sample pad to the test line and finally into the absorbent pad. Because digoxin is a small molecule with very few unique binding epitopes, a competitive assay LFA format was utilized. As the sample flows past the test line composed of immobilized digoxin-BSA, the anti-digoxigenin antibodies on the PtNPs which are not saturated with digoxin from the serum sample will be able to bind to the test line. Thus, a low concentration of digoxin in the serum results in high binding of PtNPs to the test line, while a high concentration of digoxin results in low binding of PtNPs to the test line.

A 5 mm x 5 mm section of the LFA containing the test line is then cut out and transferred into a holder above a 96-well plate, where the test line is submerged in an H_2O_2 incubation solution. It has previously been demonstrated that noble metal nanoparticles (such as those composed of gold, silver, platinum, and palladium) possess pH-switchable catalytic activities.[27] In

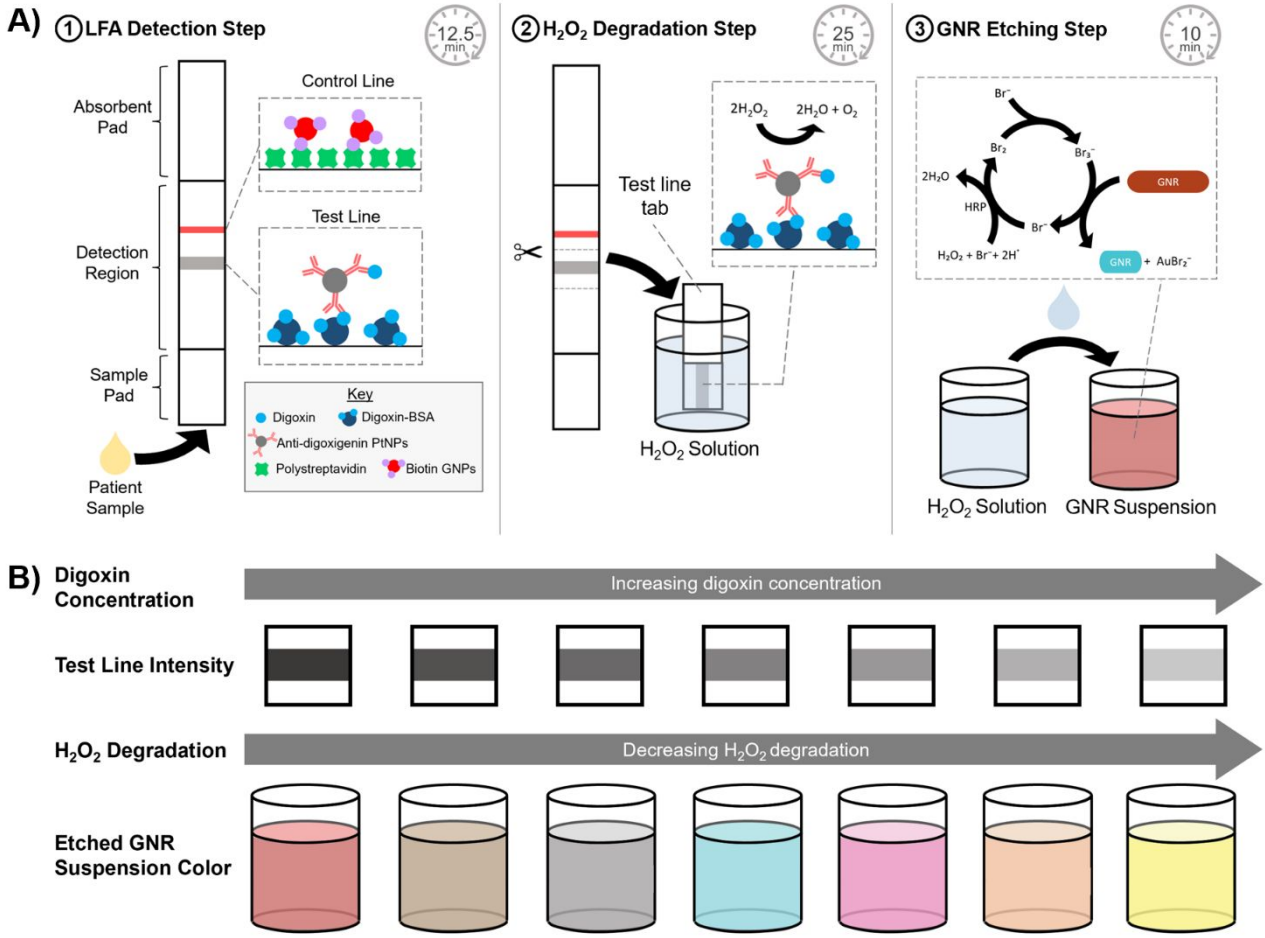

Figure 1 Simplified schematic of assay steps and resulting color output. **(A)** (1) Serum sample, control line GNPs, and test line PtNPs are applied to the LFA test strip and antigen capture occurs in the detection zone. (2) After detection, the test line is excised, rotated 90 degrees, and attached to a stabilizing tab, before being transferred to a basic H_2O_2 solution where the PtNPs bound to the test line catalyze the catalase-like degradation of H_2O_2. (3) After degradation, the H_2O_2 solution is transferred to a GNR suspension where any remaining H_2O_2 oxidizes bromide to form tribromide which leads to anisotropic etching of the GNRs. **(B)** The relationship between digoxin concentration, test line intensity, H_2O_2 degradation, and the etched GNR suspension color resulting in a semi-quantitative, multicolor readout.

acidic conditions, they possess peroxidase-like activities where they catalyze the breakdown of H_2O_2 into free radicals which can oxidize chromogenic substrates.[28] In basic conditions, the nanoparticles possess catalase-like activities, where they catalyze the degradation of H_2O_2 into water and oxygen.[29] Therefore, we chose to use a basic pH for the H_2O_2 incubation solution so that the breakdown of H_2O_2 into water and oxygen would be catalyzed by any PtNPs bound to the test line. After this incubation, the concentration of H_2O_2 remaining in the solution would be directly related to the initial digoxin concentration in the original serum sample. A low concentration of digoxin results in a high amount of PtNPs bound to the test line, fast degradation of the H_2O_2, and thus less H_2O_2 remaining. On the other hand, a high concentration of digoxin results in a low amount of PtNPs bound to the test line, slow degradation of H_2O_2, and thus, more H_2O_2 remaining.

To convert the concentration of H_2O_2 remaining in the incubation solution to the final visible multicolor readout, an oxidative GNR etching reaction is utilized. The H_2O_2 solution is transferred into a separate suspension containing GNRs, HRP, CTAB, Tween 20, and NaBr in a citrate buffer. The HRP would catalyze the oxidation of bromide ions to diatomic bromine (Br_2), which in the presence of excess bromide would be converted to the reactive species tribromide. The tribromide ions then form complexes with positively-charged cetyltrimethylammonium (CTA) micelles due to strong electrostatic interactions. It has been suggested that this interaction both stabilizes the reactive tribromide ion and facilitates the transport of the tribromide to the surface of the GNRs which are coated with a CTA bilayer.[30] The tribromide will preferentially oxidize the gold atoms on the tips of the GNRs, resulting in the anisotropic etching and shortening of the GNRs. By adding different concentrations of H_2O_2 into the GNR etching reaction, the GNRs would be etched to varying degrees, producing different sized GNRs. It is widely known that the optical properties of GNR suspensions are highly dependent on the particle aspect ratio (length divided by width) due to localized surface plasmon resonance, allowing for the production of a wide range of different colored suspensions through anisotropic etching. Ultimately, differences in the initial concentration of digoxin in the serum sample would result in GNRs being etched to different degrees that produce distinct differences in the visible color of the suspension that are easily interpreted by the naked eye.

3.2 Demonstration of GNR etching for multicolor semi-quantification of hydrogen peroxide

While the oxidative anisotropic etching of GNRs has previously been reported to produce a wide spectrum of visible colors, studies that specifically etch GNRs using H_2O_2 and HRP without 3,3',5,5'-tetramethylbenzidine have reported limited ranges in color production.[31,32] Prior to combining this reaction with the LFA, it was therefore necessary to characterize the importance of each reagent and determine the feasibility of using this reaction to produce a wide color spectrum.

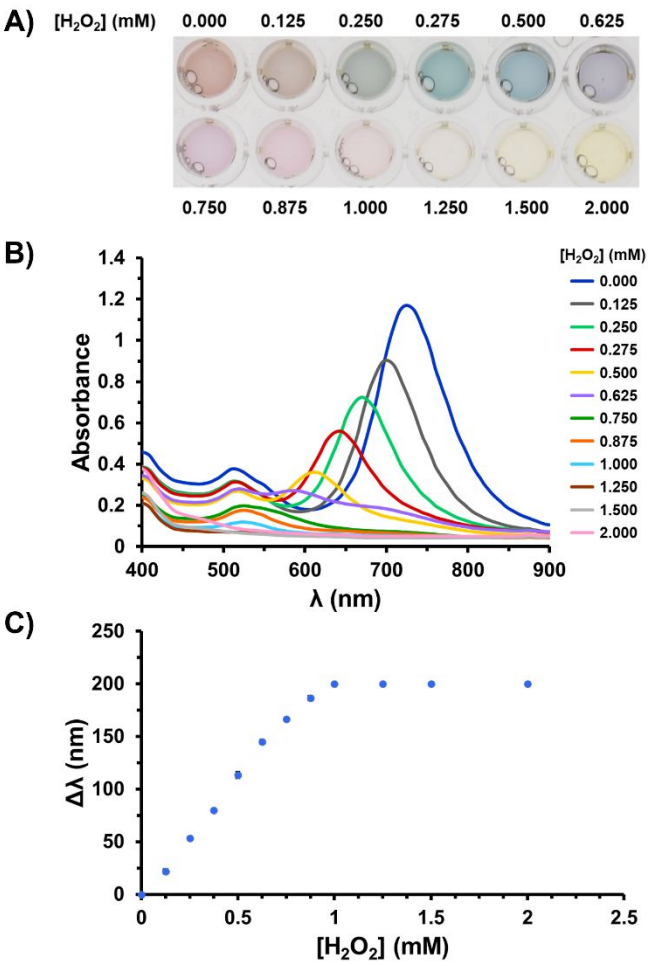

Figure 2 (A) Photographs and **(B)** UV-Vis spectra resulting from exposing GNR etching suspensions to varying concentrations of H_2O_2. **(C)** Difference in the peak wavelength value of the longitudinal plasmon band after the GNR etching reaction relative to the condition without H_2O_2 for varying concentrations of H_2O_2. All data is presented as mean ± SD (n = 3).

Initial GNR etching experiments without Tween 20 had inconsistent results due to the precipitation of CTAB out of solution at room temperature. We found that Tween 20 was able to dramatically improve the solubility of CTAB when introduced at an equal molar concentration to that of CTAB, with solutions remaining stable at 4 °C and without having a negative effect on etching (**Figure S2** in Supplementary Information). We also confirmed that the presence of H_2O_2 and HRP was necessary for any etching to occur, while the inclusion of additional bromide ions from NaBr allowed for further etching of the GNRs. Additionally, the absence of CTAB resulted in aggregation of the GNRs, while too high of a concentration of CTAB led to decreased etching (**Figure S3** in Supplementary Information). We used this information to optimize the composition of our GNR etching suspension.

To determine the full range of colors that could be produced from the GNR etching reaction, the added H_2O_2 concentration was varied from 0 to 2 mM. After reacting for 10 min, a wide spectrum of colors was produced (**Figure 2A**). Our experiment demonstrated that at least 10 distinct colors could be produced which are easily distinguishable by the naked eye. The resulting

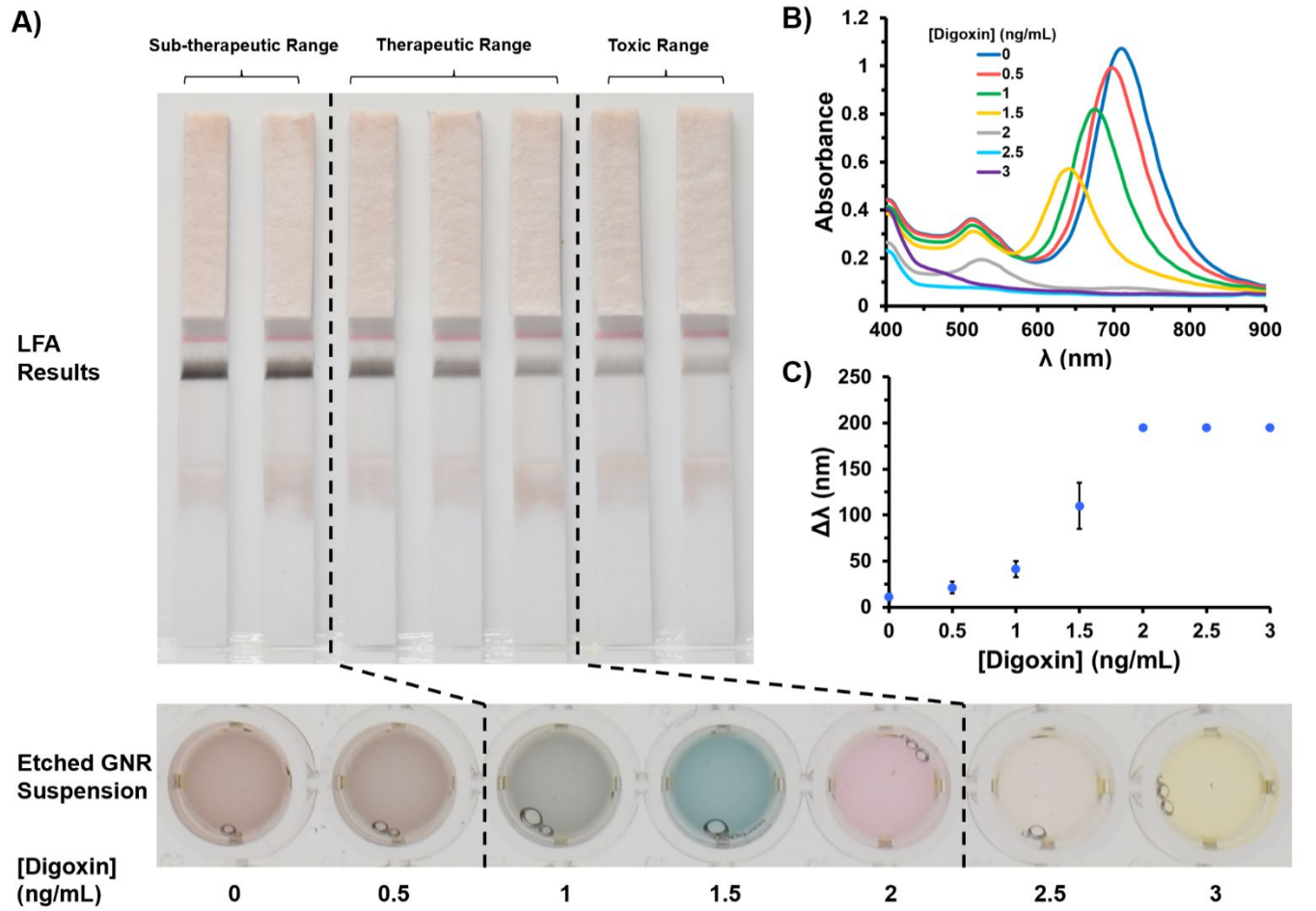

Figure 3 (A) LFA test lines and corresponding GNR suspensions resulting from the combined LFA and GNR etching reaction. LFA test line intensity decreases and GNR etching increases with an increase in digoxin concentration. Note that the control line is red instead of the gray color of the PtNPs as gold nanoparticles conjugated to BSA-biotin (GNPs) are binding to polystreptavidin on the control line. **(B)** UV-Vis spectra of the GNR suspensions. **(C)** Change in peak value of the UV-Vis longitudinal wavelength of the GNR suspensions relative to the value before the GNR etching reaction. Data is presented as mean ± SD (n = 4).

UV-Vis spectra confirmed that the GNRs are being etched, indicated by the progressive blue-shift in the longitudinal plasmon band that corresponds to a decreasing GNR aspect ratio (**Figure 2B**). The change in the longitudinal plasmon band peak wavelength was linear as a function of H_2O_2 concentration until 0.875 mM of H_2O_2 (**Figure 2C**). The resulting suspensions at 0.875 and 1 mM are pink and their corresponding UV-Vis spectra no longer have the longitudinal plasmon band that is characteristic of a GNR. It is at this point that the GNRs have become spherical gold nanoparticles and have begun to etch evenly from all sides until no nanoparticles are left in the suspension. The yellow color of the solution from etching with 1.25, 1.5, and 2 mM H_2O_2 can be attributed to the further oxidation of the GNR etching reaction product $AuBr_2^-$ into $AuBr_4^-$ once all GNRs and spherical particles are completely degraded.[13] It is worth noting that the GNR etching reaction is extremely reproducible as shown in **Figure 2C**, where most error bars are not visible due to being so small.

3.3 Semi-quantitative detection of digoxin using the LFA with a multicolor readout

We then moved on to evaluate whether our proposed assay could produce easily distinguishable colored results with small changes in digoxin concentration within the clinically relevant range of 0.5 to 3 ng/mL. The test lines produced after running the digoxin serum samples on the LFA for 12.5 min are shown in **Figure 3A**. As expected for a competitive assay format, the darkest test line is observed for the negative, and the test line intensity decreases as the concentration of digoxin increases. This indicates that there are differences in the amount of PtNPs bound to each test line for varying concentrations of digoxin, which is required for the H_2O_2 incubation step to yield different amounts of H_2O_2 that ultimately etch GNRs to varying degrees. It is important to note that it would be difficult for a user to reliably match the intensity of each line with a concentration of digoxin, especially within the higher digoxin concentration range of 2-3 ng/mL where the test line intensity differences between each condition are minor.

The resulting GNR suspensions are also shown in **Figure 3A**. It can be observed that the GNR etching reaction produced easily distinguishable colors that were dependent on the concentration of digoxin in the serum sample. This is in contrast to interpreting the test lines by intensity, where the visible differences can be slight and may be difficult to interpret quantitatively without the aid of an electronic reader. The color trend produced was also consistent with **Figure 2A**, and the UV-Vis results in **Figures 3B** and **3C** match the results from **Figures 2B** and **2C**, where decreasing digoxin concentrations result in a

progressive blue-shift in the longitudinal plasmon band. This confirms that the increased amount of PtNPs bound to the test line with the lower digoxin concentrations degraded more of the H_2O_2 in the incubation solution when compared to the higher digoxin concentrations. Though the shift in longitudinal peak plateaus after 2 ng/mL as the GNRs begin to etch from all directions, there are still distinct visual differences between 2, 2.5, and 3 ng/mL. This has also been confirmed through analysis of the RGB values of the GNR suspensions (**Figure S4** in Supplementary Information). The results can be divided into three bins: the subtherapeutic range which stretches from red to brown, the therapeutic range which stretches from grey to pink, and the toxic range which stretches from light orange to yellow. Ultimately, our assay is able to semi-quantitatively detect for digoxin in human serum by providing distinct colors below, within, and above the therapeutic window. Furthermore, not only can our assay be used to classify samples within these three categories, but it also provides more accurate measurements that have the potential to be used to calculate adjustments in dosage for individualized therapy.

This technology could be useful in the semi-quantitative detection of many other targets besides digoxin by altering various components of the assay such as PtNP conjugation, PtNP concentration, H_2O_2 degradation time, etc., to detect other biomarkers. Other therapeutic drug monitoring applications that our assay could be adapted to address include the semi-quantitative monitoring of levofloxacin for tuberculosis treatment, infliximab for inflammatory bowel diseases, antiepileptic drugs, and immunosuppressants to prevent organ rejection following transplant.[33] Besides therapeutic drug monitoring, we believe the multicolor, semi-quantitative assay developed here could find applications in environmental contaminant testing.[34] Additionally, preliminary analysis shows potential for this technology to be used at a low cost.

We acknowledge that this technique in its current stage is more complex than the conventional LFA because it requires additional handling steps, which could limit its use in at-home or in-field settings. Although certain steps could already be simplified by adopting components of commercialized LFAs—such as the dehydration of conjugates within a conjugate pad and the integration of the LFA within a user-friendly casing to reduce solution handling—the complexity of the remaining steps of the technique still limits its usability. Nevertheless, this technique could serve to bridge the gap between the simple one-step, qualitative LFA and the more complex quantitative, plasmonic ELISA. It is also the starting point for future work in the development of a fully paper-based version of this technology that facilitates both the degradation of H_2O_2 and the etching of GNRs immobilized within a paper matrix as part of a unified and standalone diagnostic device, which will minimize user steps and eliminate the need for any laboratory equipment such as pipettes or microplate shakers. Furthermore, we believe this future dehydration or immobilization of assay components onto paper will aid in improving the shelf-life of our test, which is necessary for a fully POC device.

Conclusions

In summary, we have developed a new method for the semi-quantification of digoxin concentration in serum by combining the LFA with a GNR etching reaction. To our knowledge, this is the first combination of the LFA with a GNR etching reaction, as well as the first semi-quantitative LFA with a multicolor readout that is dependent on the initial analyte concentration. We believe this work serves as a starting point for the development of a new generation of highly quantitative, lateral-flow immunoassays which can be operated without the need for expensive laboratory equipment and electronic devices since it is easier for the naked eye to discern changes in color hue versus changes in intensity of one color. Ultimately, this could lead to more effective patient management and treatment in resource-limited settings.

Author Contributions

Conceptualization: DWB, JTT, MJR, BMW, DTK. Investigation: DWB, JTT, MJR, KJC, AAB. Methodology: DWB, JTT, MJR, KJC, AAB. Formal analysis: DWB, JTT, MJR, KJC, AAB, DTK. Validation: DWB, JTT, MJR, KJC, AAB. Writing - original draft: DWB, JTT, MJR, KJC, AAB. Writing - review & editing: BMW, DTK. Funding acquisition: DTK. Project administration: DWB, JTT, MJR, DTK. Supervision: DTK. Resources: DTK.

Conflicts of interest

There are no conflicts to declare.

Acknowledgements

This project was supported by a seed grant provided by the Precise Advanced Technologies and Health Systems for Underserved Populations (PATHS-UP) Engineering Research Center (ERC) funded by the National Science Foundation (NSF) (Award No. 1648451).

References

1 C. W. Tsao, A. W. Aday, Z. I. Almarzooq, A. Alonso, A. Z. Beaton, M. S. Bittencourt, A. K. Boehme, A. E. Buxton, A. P. Carson, Y. Commodore-Mensah, M. S. V. Elkind, K. R. Evenson, C. Eze-Nliam, J. F. Ferguson, G. Generoso, J. E. Ho, R. Kalani, S. S. Khan, B. M. Kissela, K. L. Knutson, D. A. Levine, T. T. Lewis, J. Liu, M. S. Loop, J. Ma, M. E. Mussolino, S. D. Navaneethan, A. M. Perak, R. Poudel, M. Rezk-Hanna, G. A. Roth, E. B. Schroeder, S. H. Shah, E. L. Thacker, L. B. VanWagner, S. S. Virani, J. H. Voecks, N. Y. Wang, K. Yaffe and S. S. Martin, Circulation, 2022, 145, e153–e639.

2 S. S. Virani, A. Alonso, E. J. Benjamin, M. S. Bittencourt, C. W. Callaway, A. P. Carson, A. M. Chamberlain, A. R. Chang, S. Cheng, F. N. Delling, L. Djousse, M. S. V. Elkind, J. F. Ferguson, M. Fornage, S. S. Khan, B. M. Kissela, K. L. Knutson, T. W. Kwan, D. T. Lackland, T. T. Lewis, J. H. Lichtman, C. T. Longenecker, M. S. Loop, P. L. Lutsey, S. S. Martin, K. Matsushita, A. E. Moran, M. E. Mussolino, A. M. Perak, W. D. Rosamond, G. A. Roth, U. K. A. Sampson, G. M. Satou, E. B. Schroeder, S. H. Shah, C. M. Shay, N. L. Spartano, A. Stokes,

D. L. Tirschwell, L. B. VanWagner, C. W. Tsao, S. S. Wong and D. G. Heard, Circulation, 2020, 141, E139–E596.
3 P. A. Heidenreich, J. G. Trogdon, O. A. Khavjou, J. Butler, K. Dracup, M. D. Ezekowitz, E. A. Finkelstein, Y. Hong, S. C. Johnston, A. Khera, D. M. Lloyd-Jones, S. A. Nelson, G. Nichol, D. Orenstein, P. W. F. Wilson and Y. J. Woo, Circulation, 2011, 123, 933–944.
4 C. P. Mouton, M. Hayden and J. H. Southerland, Prim Care, 2017, 44, e37–e71.
5 O. J. Ziff and D. Kotecha, Trends in Cardiovascular Medicine, 2016, 26, 585–595.
6 G. Grześk, W. Stolarek, M. Kasprzak, M. Krzyżanowski, K. Szadujkis-Szadurska, M. Wiciński and E. Grześk, Pharmacol Rep, 2018, 70, 184–189.
7 R. Valdes Jr, S. A. Jortani and M. Gheorghiade, Clinical Chemistry, 1998, 44, 1096–1109.
8 J. S. Kang and M. H. Lee, Korean J Intern Med, 2009, 24, 1–10.
9 K. Aonuma, T. Shiga, H. Atarashi, K. Doki, H. Echizen, N. Hagiwara, J. Hasegawa, H. Hayashi, K. Hirao, F. Ichida, T. Ikeda, Y. Maeda, N. Matsumoto, T. Sakaeda, W. Shimizu, M. Sugawara, K. Totsuka, Y. Tsuchishita, K. Ueno, E. Watanabe, M. Hashiguchi, S. Hirata, H. Kasai, Y. Matsumoto, A. Nogami, Y. Sekiguchi, T. Shinohara, A. Sugiyama, N. Sumitomo, A. Suzuki, N. Takahashi, E. Yukawa, M. Homma, M. Horie, H. Inoue, H. Ito, T. Miura, T. Ohe, K. Shinozaki and K. Tanaka, Circ J, 2017, 81, 581–612.
10 B. Sanavio and S. Krol, Front Bioeng Biotechnol, 2015, 3, 20.
11 J. Satija, N. Punjabi, D. Mishra and S. Mukherji, RSC Advances, 2016, 6, 85440–85456.
12 L. Tang and J. Li, ACS Sensors, 2017, 2, 857–875.
13 X. Ma, Z. Chen, P. Kannan, Z. Lin, B. Qiu and L. Guo, Analytical Chemistry, 2016, 88, 3227–3234.
14 X. Ma, Y. Lin, L. Guo, B. Qiu, G. Chen, H. hao Yang and Z. Lin, Biosens Bioelectron, 2017, 87, 122–128.
15 P. Yager, G. J. Domingo and J. Gerdes, Annu Rev Biomed Eng, 2008, 10, 107–144.
16 W. Leung, C. P. Chan, T. H. Rainer, M. Ip, G. W. H. Cautherley and R. Renneberg, J Immunol Methods, 2008, 336, 30–36.
17 H. Y. Yin, P. T. Chu, W. C. Tsai and H. W. Wen, Food Chem, 2016, 192, 934–942.
18 A. E. Kita, D. W. Bradbury, Z. D. Taylor, D. T. Kamei and M. A. st. John, Otolaryngol Head Neck Surg, 2018, 159, 824–829.
19 O. Mudanyali, S. Dimitrov, U. Sikora, S. Padmanabhan, I. Navruz and A. Ozcan, Lab Chip, 2012, 12, 2678–2686.
20 J. Zhang, Z. Shen, Y. Xiang and Y. Lu, ACS Sensors, 2016, 1, 1091–1096.
21 C. Ruppert, N. Phogat, S. Laufer, M. Kohl and H. P. Deigner, Mikrochim Acta, 2019, 186, 119.
22 S. Lee, S. Mehta and D. Erickson, Analytical Chemistry, 2016, 88, 8359–8363.
23 A. N. Danthanarayana, E. Finley, B. Vu, K. Kourentzi, R. C. Willson and J. Brgoch, Analytical Methods, 2020, 12, 272–280.
24 C. W. Yen, H. de Puig, J. O. Tam, J. Gómez-Márquez, I. Bosch, K. Hamad-Schifferli and L. Gehrke, Lab on a Chip, 2015, 15, 1638–1641.
25 X. Ye, L. Jin, H. Caglayan, J. Chen, G. Xing, C. Zheng, V. Doan-Nguyen, Y. Kang, N. Engheta, C. R. Kagan and C. B. Murray, ACS Nano, 2012, 6, 2804–2817.
26 C. N. Loynachan, M. R. Thomas, E. R. Gray, D. A. Richards, J. Kim, B. S. Miller, J. C. Brookes, S. Agarwal, V. Chudasama, R. A. McKendry and M. M. Stevens, ACS Nano, 2018, 12, 279–288.
27 J. Li, W. Liu, X. Wu and X. Gao, Biomaterials, 2015, 48, 37–44.
28 Y. Liu, H. Wu, M. Li, J. J. Yin and Z. Nie, Nanoscale, 2014, 6, 11904–11910.
29 Z. Zhu, Z. Guan, S. Jia, Z. Lei, S. Lin, H. Zhang, Y. Ma, Z. Q. Tian and C. J. Yang, Angew Chem Int Ed Engl, 2014, 53, 12503–12507.
30 Q. Zhu, J. Wu, J. Zhao and W. Ni, Langmuir, 2015, 31, 4072–4077.
31 L. Saa, M. Coronado-Puchau, V. Pavlov and L. M. Liz-Marzán, Nanoscale, 2014, 6, 7405–7409.
32 L. Saa, R. Grinyte, A. Sánchez-Iglesias, L. M. Liz-Marzán and V. Pavlov, ACS Applied Materials and Interfaces, 2016, 8, 11139–11146.
33 D. J. Touw, C. Neef, A. H. Thomson and A. A. Vinks, Ther Drug Monit, 2005, 27, 10–17.
34 N. A. Meredith, C. Quinn, D. M. Cate, T. H. Reilly, J. Volckens and C. S. Henry, Analyst, 2016, 141, 1874–1887.

